Analysis by kinetic modeling of the temperature dependence of thermal electron attachment to CF3Br

Jürgen Troe, Thomas M. Miller, Nicholas S. Shuman, and Albert A. Viggiano

Citation: J. Chem. Phys. **137**, 024303 (2012); doi: 10.1063/1.4729369
View online: http://dx.doi.org/10.1063/1.4729369
View Table of Contents: http://jcp.aip.org/resource/1/JCPSA6/v137/i2
Published by the American Institute of Physics.

Analysis by kinetic modeling of the temperature dependence of thermal electron attachment to CF_3Br

Jürgen Troe,[1,2,3] Thomas M. Miller,[4] Nicholas S. Shuman,[4] and Albert A. Viggiano[4]
[1]*Institut für Physikalische Chemie, Universität Göttingen, Tammannstrasse 6, D-37077 Göttingen, Germany*
[2]*Max-Planck-Institut für Biophysikalische Chemie, Am Fassberg 11, D-37077 Göttingen, Germany*
[3]*Laser-Laboratorium Göttingen, Hans-Adolf-Krebs-Weg 1, D-37077 Göttingen, Germany*
[4]*Air Force Research Laboratory, Space Vehicles Directorate, Kirtland Air Force Base, New Mexico 87117-5776, USA*

(Received 9 March 2012; accepted 30 May 2012; published online 10 July 2012)

Experimental data from the literature for cross sections and rate constants for dissociative electron attachment to CF_3Br, with separately varied electron and gas temperatures, are analyzed by a kinetic modeling approach. The analysis suggests that electronic and nuclear contributions to the rate constants can be roughly separated, the former leading to a negative temperature coefficient, the latter to a positive temperature coefficient. The nuclear factor in the rate constant is found to be of Arrhenius form with an activation energy which is close to the energy of crossing of the CF_3Br and CF_3Br^- potential curves along the CBr bond. © *2012 American Institute of Physics*. [http://dx.doi.org/10.1063/1.4729369]

I. INTRODUCTION

Electron attachment to neutral molecules is a complicated process being characterized by an interplay of electronic and nuclear motions. In two previous articles[1,2] we have tried to separate the two contributions within the framework of a "kinetic modeling,"[3] such that the temperature dependence of thermal attachment rate constants $k_{at}(T_{gas} = T_{el})$ can be represented in a simplified manner (T_{gas} = gas temperature, T_{el} = electron temperature). It was suggested that the electronic part of the problem leads to negative temperature coefficients while a nuclear threshold part leads to positive temperature coefficients such that the combination of the two contributions can result in a great variety of overall temperature dependences, see examples documented in Refs. 1–7.

The proposition of a separation of electronic and nuclear contributions to k_{at}, and of different temperature coefficients of the two factors, is not new. For example, k_{at} for dissociative electron attachment (DEA) to CF_3Br in Ref. 8, by varying electron temperatures T_{el} between 300 and 3000 K at fixed $T_{gas} = 300$ and 520 K, was shown to behave in the described way. In the meantime, DEA to CF_3Br has been studied in much larger detail, see, e.g., Ref. 9. This allows one to further inspect the proposition and proceed to a separate analysis of the electronic and nuclear contributions. This is the aim of the present article.

Our treatment of the electronic factor in k_{at} is based on extended Vogt-Wannier electron capture models (VW) in approximate analytical form.[10–13] The results of this treatment are useful reference values, being close to upper limit attachment cross sections σ_{at} and rate constants k_{at}. Metastable or unstable anion formation, however, generally is only achieved for some fraction P of the capture events, being related to "electron-phonon coupling," i.e., interaction between electronic and nuclear motions. In Refs. 1–3, P was determined empirically by comparing results from extended VW electron capture theory with experimental data. However, R-matrix theoretical models or zero-range potential treatments[4,7,14–17] are also available which at least semiquantitatively explain the properties of the empirical electron-phonon coupling factors P.

In the analysis of experimental cross sections σ_{at} and rate constants k_{at} for electron attachment to SF_6 we found that P can be approximately represented by[17]

$$P(\kappa) = P^{IVR}(\kappa) \approx \exp(-c_1\kappa), \tag{1.1}$$

where

$$k = \mu e(2\alpha E_{el})^{1/2}/\hbar^2 \tag{1.2}$$

is the reduced wave vector of the electronic motion (μ = reduced mass ≈ electron mass, α = polarizability of the neutral, and E_{el} = kinetic energy of the electron) and c_1 was found[3] to be a temperature (T_{gas}) dependent parameter (an expression $P(k) \approx \exp(-c_1\kappa^2)$ was tested in Refs. 1 and 3, but Eq. (1.1) appears to be slightly more appropriate[17]). At energies somewhat below and above the threshold for inelastic vibrational excitation of the target, a factor P^{VEX}, which also decreases with increasing E_{el}, was found to be necessary in addition,

$$P(\kappa) = P^{IVR}(\kappa)P^{VEX}(\kappa), \tag{1.3}$$

where $P^{VEX} = 1$ for $\kappa < \kappa_{\nu_1}$ and

$$P^{VEX}(\kappa) \approx \exp[-c_2(\kappa - \kappa_{\nu_1})] \tag{1.4}$$

for $\kappa \geq \kappa_{\nu_1}$ where κ_{ν_1} corresponds to the threshold energy ν_1 for inelastic vibrational excitation[17] (an expression $P^{VEX}(\kappa) \approx \exp[-c_2(\kappa^2 - \kappa_{\nu_1}^2)]$ was tested in Ref. 3, but Eq. (1.4) appears to be more appropriate[17]). Eqs. (1.1)–(1.4) were found empirically by comparing experimental data with extended Vogt-Wannier capture theory. The factor $P^{IVR}(\kappa)$ was historically related to "intramolecular vibrational relaxation"

of the excitation of an electron-accepting mode into other modes of the anion (which explains its superscript IVR). However, the term IVR certainly is misleading as the incoming electron essentially becomes integrated into the electronic shell of the neutral during fractions of one vibrational period of the accepting modes, regardless whether short-lived or long-lived anionic states are formed. In addition, influences of the possibility for vibrational excitation become noticeable below the corresponding threshold such that a separation of P into $P^{IVR}(\kappa)$ and $P^{VEX}(\kappa)$ cannot be made rigorously.[4,14,17] Nevertheless, Eqs. (1.1)–(1.4) present a most useful tool for a kinetic modeling of the overall process.[1–7]

In order to understand the dependence of the process on the electronic energy E_{el} and on T_{gas}, the additional dependence of $P(\kappa)$ on the vibrational states of the neutral (represented by a set of quantum numbers symbolized by i) needs to be addressed. If there is an energy barrier E_0 of the crossing of the multi-dimensional potential energy surfaces of the neutral and the anion, this may result in an additional factor $P_{nucl}^{IVR}(i)$ in P with a strong dependence on i. To a first approximation, we represent this by a step function with $P_{nucl}^{IVR}(i)$ becoming unity above the threshold (if more is known, Landau-Zener type expressions and tunnelling contributions may be included). $P^{IVR}(\kappa)P^{VEX}(\kappa)$ may also depend on i. However, this dependence will disappear in the low energy Bethe-limit[11,17] such that we assume it to be much weaker than expressed by $P_{nucl}^{IVR}(i)$. Tentatively, the electronic and nuclear contributions in Refs. 1 and 2 were separated in the form

$$P(E_{el}, i) \approx P_{el}^{IVR}(E_{el})\, P_{el}^{VEX}(E_{el})\, P_{nucl}^{IVR}(i), \qquad (1.5)$$

where $P_{el}^{IVR}(E_{el})\, P_{el}^{VEX}(E_{el})$ again were assumed to be given by Eqs. (1.1) and (1.4). However, now the parameters c_1 and c_2 were taken as independent or only weakly dependent of the gas temperature, and, hence, of the vibrational quantum state i of the neutral. On the other hand, the factor $P_{nucl}^{IVR}(i)$ related to a nuclear threshold energy was assumed to depend more strongly on i. Whether Eq. (1.5) is a good approximation remains to be examined by experiments. This is one of the aims of the present study.

Averaging the product of the attachment cross section and the velocity over the respective distributions of electron velocities and states i of the neutral leads to the attachment rate constants. With thermal electrons of temperature T_{el} and thermal populations of the vibrational states i of the neutral at gas temperature T_{gas}, Eq. (1.5) results in a rate constant of the form

$$k_{at}(T_{el}, T_{gas}) \approx k_{at}(T_{el})F(T_{gas}), \qquad (1.6)$$

such as observed, e.g., in Ref. 8 for DEA to CF_3Br, i.e., in the reaction

$$CF_3Br + e^- \rightarrow CF_3 + Br^-. \qquad (1.7)$$

Experiments with separate variation of T_{el} and T_{gas} thus allow one to test Eqs. (1.5) and (1.6). If, in addition, attachment cross sections at fixed T_{gas} are measured as a function of E_{el}, the validity of a representation

$$\sigma_{at}(E_{el}) \approx \sigma_{at}^{VW}(E_{el})\, P_{el}^{IVR}(E_{el})\, P_{el}^{VEX}(E_{el})\, P_{nucl}^{IVR}(i) \qquad (1.8)$$

with $P_{el}^{IVR}(E_{el})\, P_{el}^{VEX}(E_{el})$ given by Eqs. (1.1) and (1.4) can be tested as well and the parameters c_1 and c_2 can be derived. Finally, models for $P_{nucl}^{IVR}(i)$ can be tested by means of experimental determinations of the factor $F(T_{gas})$.

A series of experimental systems now are available to perform the described type of analysis, see, e.g., Ref. 6. Among the studied reactions, DEA to CF_3Br appears particularly suitable because the experimental database is extensive (see Ref. 9 and earlier work cited therein) and R-matrix calculations have also been made.[6,7,9] The work of Ref. 9 in particular provides what is needed for this type of analysis. Measurements of $k_{at}(T_{el},T_{gas})$ with separate variation of T_{el} and T_{gas} over the ranges 300–20 000 K and 173–600 K, respectively, and measurements of $\sigma_{at}(E_{el})$ over the range 1–2000 meV at $T_{gas} = 300$ K were made. The measurements of $\sigma_{at}(E_{el})$ were detailed enough to characterize the product $P_{el}^{IVR}P_{el}^{VEX}$ in Eq. (1.5). A separation into P_{el}^{IVR} and P_{el}^{VEX} would only be essential when attachment and detachment properties are to be linked by detailed balancing.[18] Using the experimental data for DEA to CF_3Br as first example, our article hopes to motivate further tests of the validity of Eq. (1.5). Furthermore, the separate forms of $P_{el}^{IVR}(E_{el})\, P_{el}^{VEX}(E_{el})$ and $P_{nucl}^{IVR}(i)$ are of interest because, together with the known expressions for extended Vogt-Wannier reference values of k_{at}^{VW} and σ_{at}^{VW}, they provide a simple access to a general analysis of the temperature dependence of thermal attachment rate constants k_{at}.

II. ANALYSIS OF EXPERIMENTAL RATE CONSTANTS AND CROSS SECTIONS: ELECTRONIC CONTRIBUTIONS

DEA rate constants for CF_3Br as a function of electron and gas temperatures, T_{el} and T_{gas}, respectively, first are analyzed by considering experimental ratios of $k_{at}(T_{el}, T_{gas})/k_{at}(T_{el} = 500\text{K}, T_{\text{gas}})$ for a range of fixed T_{gas} values. The analysis of rate constant ratios has the advantage that the appropriateness of a factorized representation like Eq. (1.6) can immediately be tested. The microwave cavity pulse radiolysis with microwave heating data from Ref. 9 (MWPR-MH) and the flowing afterglow with Langmuir probe data from Ref. 8 (FALP) are used to derive this ratio. Fig. 1 shows the results. The obtained ratios apparently all roughly fall on one curve, although the experimental scatter admittedly is rather large. The representation used $k_{at}(T_{el} = 500\text{ K}, T_{gas})/10^{-8}$ cm^3 s^{-1} = 0.18, 0.31, 1.05, 4.8, 5.5, and 9.1 for $T_{gas} = 173$, 223, 300, 450, 520, and 600 K, respectively, such as derived by interpolation and extrapolation of the data from Ref. 9. Within the scatter this suggests that Eq. (1.6) holds and that the nuclear factor $F(T_{gas})$ does not depend on T_{el}. The ratio shown in Fig. 1 then reduces to $k_{at}(T_{el})/k_{at}(T_{el} = 500\text{ K})$ independent of T_{gas}.

We remember that the electronic contribution $k_{at}(T_{el})$ to k_{at} is given by[11]

$$k_{at}(T_{el}) = k_L \int_0^\infty P^{VW}(\kappa) P_{el}^{IVR}(\kappa)\, P_{el}^{VEX}(\kappa)\, f(\kappa, \theta_{el})\, d\kappa/2\kappa \qquad (2.1)$$

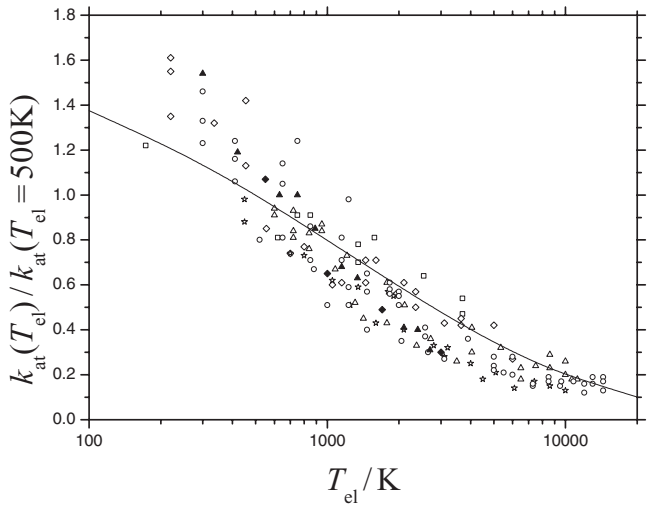

FIG. 1. Thermal rate constants for DEA to CF_3Br with separated electron and gas temperatures T_{el} and T_{gas}, respectively. Reduced representation relative to $k_{at}(T_{el} = 500\ \mathrm{K})/10^{-8}\ \mathrm{cm^3\ s^{-1}} = 0.18, 0.31, 1.05, 4.8, 5.5$, and 9.1 for $T_{gas} = 173$, 223, 300, 450, 520, and 600 K, respectively. (Experimental points: T_{gas}/K = 173 (□), 223 (◇), 300 (○), 450 (☆), and 600 (△) from Ref. 9; 300 (▲) and 520 (◆) from Ref. 8; full line: kinetic modeling from this work based on cross section measurements at $T_{gas} = 300$ K from Ref. 9, see text.)

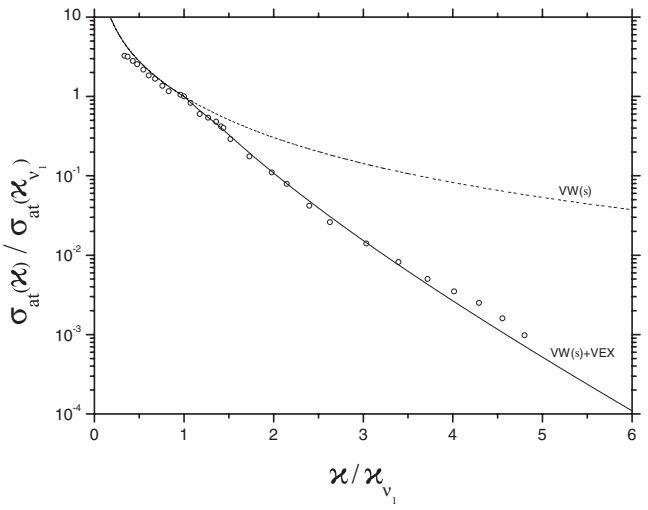

FIG. 2. Cross sections for DEA to CF_3Br at $T_{gas} = 300$ K. Reduced representation relative to $\sigma_{at}(E_{el} = \nu_1 = 43.4\ \mathrm{meV}) \approx 1.2 \times 10^{-17}\ \mathrm{cm^2}$. (Selection of experimental points ○ from Ref. 9; dashed curve VW(s): extended Vogt-Wannier electron capture theory for s-wave electrons with Eq. (2.5); full curve: VW(a) + VEX: as VW(s), but with IVR factors from Eqs. (1.1), (1.4) and (2.7), see text.)

with the Langevin rate constant

$$k_L = 2\pi e(\alpha/\mu)^{1/2}, \tag{2.2}$$

the reduced wave vector κ from Eq. (1.2), the reduced electron temperature

$$\theta_{el} = k_B T_{el} \alpha e^2 \mu^2/\hbar^4, \tag{2.3}$$

and the thermal distribution

$$f(k, \theta_{el}) = \left[2k^2/(2\pi)^{1/2}\theta_{el}^{3/2}\right] \exp(-k^2/2\theta_{el}). \tag{2.4}$$

The Vogt-Wannier capture probability, for s-wave electrons and non-polar neutrals, is approximated by[11,13]

$$P^{VW}(k) \approx 1 - 0.25\exp(-1.387k) - 0.75\exp(-4.871k). \tag{2.5}$$

As will be shown later, however, the contributions from higher partial waves (p- and d-waves) to $P^{VW}(\kappa)$ should also be taken into consideration. These are treated by the analytical approximations elaborated in Refs. 11–13.

If $P(\kappa)$ would exclusively be represented by Eq. (1.1), the ratio $k_{at}(\theta_{el})/k_{at}(\theta_{el} = 0.0716)$ could be used directly to extract the parameter c_1 ($\theta_{el} = 0.0716$ for the CF_3Br-system corresponds to $T_{el} = 500$ K, see below). However, with increasing energy the factor $P^{VEX}(\kappa)$ increasingly falls below unity, see Refs. 4, 7, 14–17. As this factor markedly decreases below unity only at E_{el} above some threshold value ν_1, its influence becomes important only at large values of θ_{el} and cannot be recovered from Fig. 1. A better access to P_{el}^{VEX} is provided by direct measurements of energy-resolved attachment cross sections σ_{at} such as also performed in Ref. 9. These experiments show changes of the slope of $\sigma_{at}(E_{el})$ at $E_{el} = \nu_1$ and $E_{el} = 2\nu_1$ where $\nu_1 = 43.4$ meV is one quantum of the C-Br stretching mode in CF_3Br. In order to derive the corresponding factors $P_{el}^{IVR}(\kappa)$ and $P_{el}^{VEX}(\kappa)$ from the experimental cross sections σ_{at}, the Vogt-Wannier expression has to be specified. The expression for $k_{at}(T_{el})$ of Eq. (2.1) corresponds to cross sections of the form

$$\sigma_{at}(\kappa) = \frac{\pi\mu e^2\alpha}{\hbar^2\kappa^2} P^{VW}(\kappa)\, P^{IVR}(\kappa)\, P^{VEX}(\kappa) \tag{2.6}$$

with κ given by Eq. (1.2). Employing a polarizability of CF_3Br $\alpha = 6.7 \times 10^{-24}\ \mathrm{cm^3}$ (interpolated value from Ref. 8), κ is related to E_{el} by $\kappa = 1.82\sqrt{E_{el}/eV}$ such that $E_{el} = \nu_1$ corresponds to $\kappa_{\nu_1} = 0.38$ and $E_{el} = 2\nu_1$ to $\kappa_{\nu_1}\sqrt{2} = 0.54$. The factor $\pi\mu\, e^2\alpha/\hbar^2$ in Eq. (2.6) has a value of $3.96 \times 10^{-15}\ \mathrm{cm^2}$. For an unpolar neutral and s-waves, $P^{VW}(\kappa)$ would be given by Eq. (2.5). However, the polar character of CF_3Br needs further consideration. With a dipole moment $\mu_D = 0.65$ D from Ref. 19, the reduced dipole moment $d = e\mu\mu_D/\hbar^2$ has a value of 0.26. As experimental determinations of σ_{at} have been made[9] for $E_{el} > 5$ meV, this corresponds to a range of $\kappa > 0.13$. Inspecting Fig. 2 of Ref. 13 then indicates that $P^{VW}(\kappa)$, for s-waves, within better than 2% still is given by Eq. (2.5).

Proceeding with the given molecular parameters to the analysis of experimental cross sections, we avoid the problem of calibrating absolute values of σ_{at} by again looking at relative cross sections $\sigma_{at}(E_{el})/\sigma_{at}(E_{el} = \nu_1)$ obtained for $T_{gas} = 300$ K in Ref. 9. This ratio in Fig. 2 then is plotted as a function of the ratio $\kappa/\kappa_{\nu_1} = \sqrt{E_{el}/\nu_1}$ and it is compared with $P^{VW}(\kappa/\kappa_{\nu_1})/P^{VW}(\kappa/\kappa_{\nu_1} = 1)$. As mentioned above, the s-wave expression of Eq. (2.5) for Vogt-Wannier reference cross sections suffices only for low energies. At energies such as covered in Fig. 2, also p- and d-wave contributions have to be considered. We have done this by using the expressions from Refs. 11–13. By showing VW results for s-wave (in Fig. 2) and for s+p+d-wave contributions (in Fig. 3), the effects are illustrated. While, within the VW approach, σ_{at} ($E_{el} = 1$ meV) for s-waves is only about 0.1% smaller than

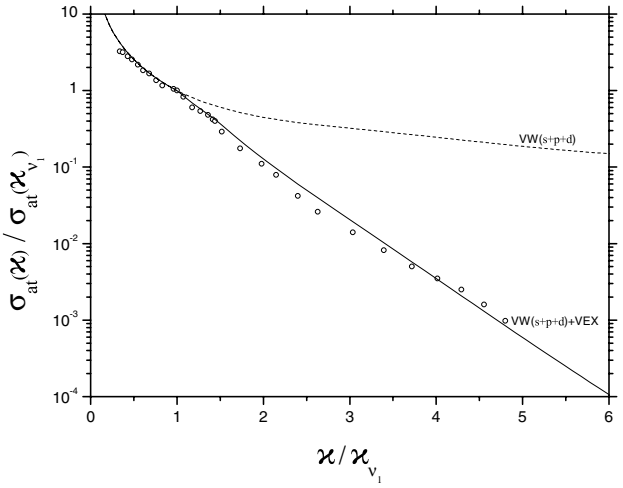

FIG. 3. As Fig. 2, but for s+p+d-wave electrons (see text).

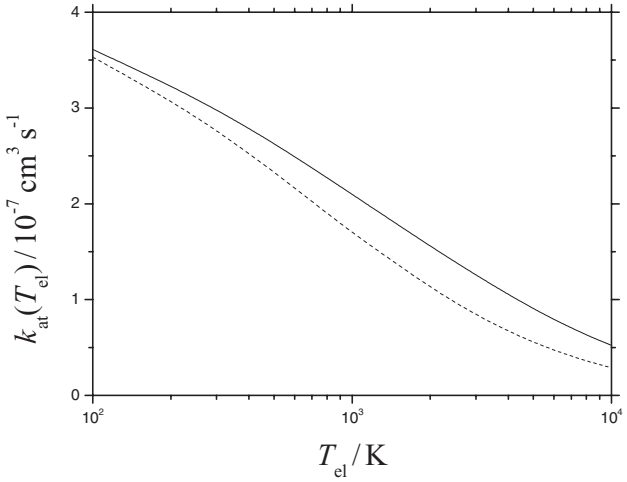

FIG. 4. Electronic contribution $k_{at}(T_{el})$ to the rate constant for DEA to CF_3Br (dashed curve: kinetic modeling for s-wave electrons, full curve; kinetic modeling for s+p+d-wave electrons; electron-phonon coupling factors P^{IVR} from the analysis of attachment cross sections at $T_{gas} = 300$ K of Ref. 9, see text).

for s+p+d-waves, it is about 10% smaller at $E_{el} = \nu_1 = 43$ meV and about a factor of 3.8 smaller at $E_{el} = 1$ eV such that contributions from higher waves should at least be taken into consideration (see below). This situation is not much different from electron attachment to $POCl_3$ where s+p+d-waves are required to describe attachment cross sections above energies of about 50 meV, see Ref. 20. It has been argued[9] that higher partial waves for symmetry reasons do not contribute to DEA to CF_3Br. As in our work quite generally we use extended VW capture theory with all partial waves as the reference, contributions from higher partial waves then would have to be reduced by small, individual, partial wave IVR-factors, see below.

Comparing the experimental cross section ratios in Figs. 2 and 3 with the Vogt-Wannier results, the parameters c_1 from Eq. (1.1) and c_2 from Eq. (1.4) can be fitted. In doing this, there is first the problem that the slope of the experimental data for $\kappa/\kappa_{\nu_1} < 1$ is somewhat smaller than given by the Vogt-Wannier approach which would result in $c_1 < 0$. We attribute this to experimental uncertainties and put $c_1 \approx 0$. Furthermore, one observes two thresholds for inelastic vibrational excitation, at κ_{ν_1} and $\kappa_{\nu_1}\sqrt{2}$ such that P_{el}^{VEX} from Eq. (1.4) has to be extended to include a second factor $P_{el,2}^{VEX}$ which is unity for $\kappa < \kappa_{\nu_1}\sqrt{2}$ and equal to

$$P_{el,2}^{VEX} \approx \exp[-c_3(\kappa - \kappa_{\nu_1}\sqrt{2})] \tag{2.7}$$

for $\kappa > \kappa_{\nu_1}\sqrt{2}$. The fitted parameters then are $c_1 \approx 0$, $c_2 \approx 0.8$, and $c_3 \approx 0.4$ when only s-waves are considered (see Eq. (2.5)) or $c_1 \approx 0$, $c_2 \approx 0.9$, and $c_3 \approx 0.6$ when s+p+d-waves are employed with equal weight (see Refs. 11–13). The comparison of the fits of Figs. 2 and 3 to the experiments (with Fig. 2 excluding and Fig. 3 including p- and d-waves) gives equally good agreement, i.e., it does not provide clues on the true contributions from higher partial waves.

Thermal averaging of the cross sections, assuming temperature independent parameters c_1, c_2, and c_3, leads to $k_{at}(T_{el})$ such as shown in Fig. 4 without and with contributions from higher partial waves. At the same time, the corresponding ratio $k_{at}(T_{el})/k_{at}(T_{el} = 500\ \text{K})$, for s+p+d-waves, is included in Fig. 1. Fig. 4 demonstrates at which temperatures the contributions of higher partial waves to k_{at} become noticeable. While p- and d-partial waves contribute to k_{at} only about 2% at $T_{el} = 100$ K and 8% at $T_{el} = 300$ K, they increase the modeled $k_{at}(T_{el})$ by a factor of 1.28 at $T_{el} = 1000$ K and 2.28 at $T_{el} = 10\,000$ K. Furthermore, the extent of internal consistency of the analysis of rate constants and cross sections is illustrated by the comparison between experimental and modeled $k_{at}(T_{el})/k_{at}(T_{el} = 500\text{K})$ in Fig. 1. In this case the modeled ratio is obtained from the analysis of the cross section measurements at 300 K and the experimental ratio stems from the rate data for $k_{at}(T_{el},T_{gas})$. In view of the fact that two different types of experiments are compared, the extent of agreement appears satisfactory. Nevertheless, the small discrepancy between the line and the points in Fig. 1 may indicate an additional, minor, dependence of the parameters c_1, c_2, and c_3 on the gas temperature (c_1, c_2, and c_3 being determined from experiments at 300 K only). However, the major dependence on T_{gas} apparently is due to a nuclear factor as given in Eq. (1.6).

III. ANALYSIS OF EXPERIMENTAL RATE CONSTANTS: NUCLEAR CONTRIBUTIONS

The analysis and fitting of the electronic contributions to $\sigma_{at}(E_{el})$ and $k_{at}(E_{el})$ performed in Sec. II allows one to determine also the nuclear factor $F(T_{gas})$ from $k_{at}(T_{el}, T_{gas}) = k_{at}(T_{el})F(T_{gas})$, see Eq. (1.6). Combining the value $k_{at}(T_{el} = 500\ \text{K}) = 2.63 \times 10^{-7}\ \text{cm}^3\ \text{s}^{-1}$ from Fig. 4 with the interpolated and extrapolated experimental data from Ref. 9, as given in the first paragraph of Sec. II, leads to the results plotted in Fig. 5. Within the considerable experimental scatter, as illustrated also by Fig. 1, the data (for $T_{gas} \geq 170$ K) follow an Arrhenius relationship

$$F(T) \approx \exp(-920\ \text{K}/T_{gas}) \tag{3.1}$$

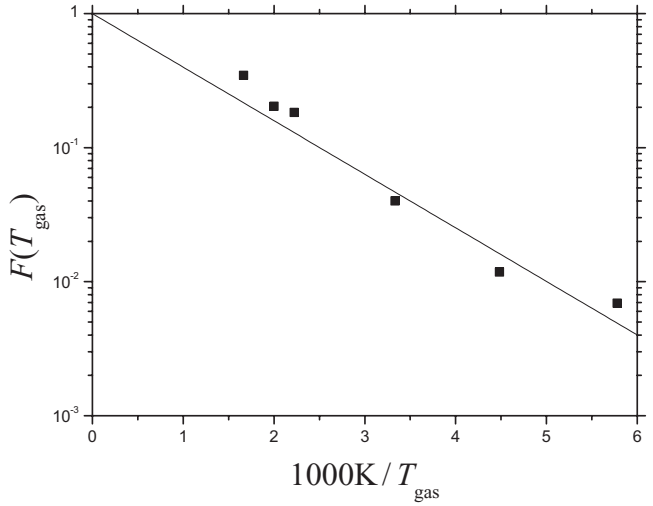

FIG. 5. Nuclear contribution $F(T_{gas})$ to the rate constant for DEA to CF_3Br (experimental points ■ based on Fig. 16 of Ref. 9 and $k_{at}(T_{el})$ from Fig. 4, see text; full line: representation by Eq. (3.1)).

with an apparent activation energy $E_a = k_B$ 920 K = 79 meV. This value within experimental uncertainty corresponds to two quanta of the C-Br stretching mode. One should note that a crossing of the neutral and anionic potential curves of CF_3Br and CF_3Br^- along the C-Br bond in Ref. 9 was estimated to occur at an energy of the order of three quanta of this mode. This at least semiquantitative agreement appears satisfactory enough. However, the crossing does not necessarily correspond to the C-Br stretch but could also involve several bonds in a multi-dimensional crossing seam.

In previous comparisons of theoretical results with experimental rate data, the factorization of $k_{at}(T_{el})$ and $F(T_{gas})$ was not used, but rather measured $k_{at}(T_{el},T_{gas} = T_{el})$ were compared with theory, see Refs. 7 and 9. Once $k_{at}(T_{el})$ and $F(T_{gas})$ are determined separately, with our analysis one easily can also recombine these quantities into the product $k_{at}(T_{el},T_{gas} = T_{el})$. This is done in Fig. 6, where the experiments selected in Fig. 2 of Ref. 7, the results from R-matrix theory of Ref. 9, and the present product of $k_{at}(T_{el})$ and $F(T_{gas} = T_{el})$ are compared. Again the general agreement appears satisfactory, if a few points are noted. The low temperature results (at 1000 K/$T_{gas} > 7.5$, corresponding to $T_{gas} < 135$ K) from Ref. 21 apparently are in error because they correspond to hot, not yet thermalized, electrons;[9,22] the open circles in Fig. 6 thus might be moved toward the left by an unknown amount. The Arrhenius plot of Fig. 5 does not include data at temperatures down to the range where the R-matrix results level off. At the highest temperatures shown in Figs. 5 and 6 the measured points are slightly above the modeled results from the present work represented by Eq. (3.1); this may or may not be relevant. Finally, the modeling results from the present analysis appear to be closer to the experimental data than the results from R-matrix theory. It should be mentioned that the latter also involve the fit of some intrinsic parameters. In the present work, there are three fit parameters (c_2, c_3, and E_a) which are directly related to attachment cross sections and thermal rate constants.

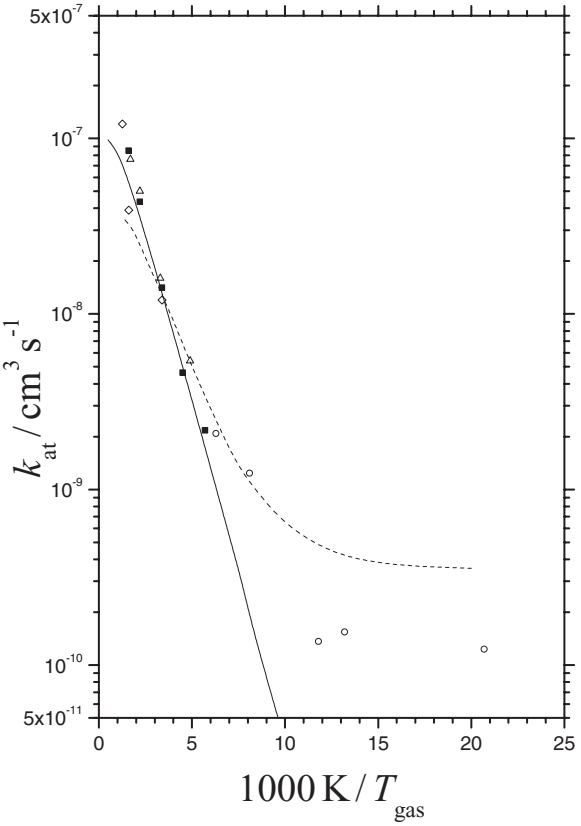

FIG. 6. Rate constants for DEA to CF_3Br at $T_{gas} = T_{el}$ (experimental points from Ref. 21 (○) being upper limits,[7,24] Ref. 9 (■), Ref. 23 (△), and Ref. 24 (◇); dashed curve: R-matrix theory from Refs. 7 and 9; full curve: kinetic modeling of this work with Eqs. (1.4), $k_{at}(E_{el})$ from full curve of Fig. 4 and $F(T)$ from Eq. (3.1), see text).

IV. CONCLUSIONS

Our kinetic modeling analysis of electron attachment to CF_3, SF_6, SF_5Cl, $POCl_3$, and CF_3Br from Refs. 1 and 2 and the present work tentatively assumes that the attachment probabilities P^{IVR} can be factorized into predominantly electronic contributions $P_{el}^{IVR}P_{el}^{VEX}$ and nuclear contributions P_{nucl}^{IVR}, see Eq. (1.5). Within experimental uncertainty this assumption is confirmed by the present analysis for DEA to CF_3Br. Of particular interest is the nuclear contribution which, after thermal averaging, leads to an Arrhenius factor $F(T_{gas})$ in the rate constant $k_{at}(T_{el},T_{gas})$ with an activation energy E_a corresponding to two quanta of the C-Br stretching mode of the neutral CF_3Br. Crossing (or avoided crossing) of the potential curves of CF_3Br and CF_3Br^- in Ref. 9 by quantum-chemical methods was calculated to occur near to three quanta of the stretching mode which is not too far away from E_a. The temperature dependence of the rate constant for DEA to CF_3Br thus can be rationalized at least semiquantitatively. It is determined by the counteraction of the electronic contribution with a negative temperature coefficient and the nuclear contribution with a positive temperature coefficient.

Similar general conclusions were drawn in Refs. 1 and 2. In particular, it was concluded that electron attachment to SF_6 also involves the overcoming of a small potential energy barrier in the nuclear coordinates. Because of similar uncertainties with experiments at temperatures below 200 K, it was

uncertain whether the nuclear factor in k_{at} follows an Arrhenius law like Eq. (3.1) or whether more complicated behavior is observed. If the latter, one possible cause is that the crossing between the potential surfaces of the neutral and the anion has multi-dimensional character. Furthermore, the representation of the nuclear IVR factor $P_{nucl}^{IVR}(i)$ in Eq. (1.5) by a Franck-Condon factor of zero at $E_{nucl} < E_a$ and unity at $E_{nucl} \geq E_a$, which corresponds to Eq. (3.1), certainly will be oversimplified. Nevertheless, the present simple results may provide a first step to a more detailed general understanding of the temperature dependence of electron attachment processes in terms of a kinetic modeling approach.

ACKNOWLEDGMENTS

Extensive discussions of this work with E. E. Nikitin and H. Hotop are gratefully acknowledged. Technical assistance by A. I. Maergoiz and G. Marowsky as well as financial support by the EOARD (Grant Award FA8655-11-3077) are acknowledged as well. This project was also supported by the (U.S.) Air Force Office of Scientific Research (USAFOSR) under Project AFOSR-2303EP. T.M.M. is under contract (FA8718-10-C-0002) to Boston College.

[1]N. S. Shuman, T. M. Miller, J. F. Friedman, A. A. Viggiano, A. I. Maergoiz, and J. Troe, J. Chem. Phys. **135**, 054306 (2011).
[2]J. Troe, G. Marowsky, N. S. Shuman, T. M. Miller, and A. A. Viggiano, Z. Phys. Chem. **225**, 1405 (2011).
[3]J. Troe, T. M. Miller, and A. A. Viggiano, J. Chem. Phys. **127**, 244303 (2007).
[4]H. Hotop, M.-W. Ruf, M. Allan, and I. I. Fabrikant, Adv. At., Mol., Opt. Phys. **49**, 85 (2003).
[5]T. M. Miller, Adv. At., Mol., Opt. Phys. **51**, 299 (2005).
[6]M.-W. Ruf, M. Braun, S. Marienfeld, I. I. Fabrikant, and H. Hotop, J. Phys. Conf. Ser. **88**, 012013 (2007).
[7]I. I. Fabrikant and H. Hotop, J. Chem. Phys. **128**, 124308 (2008).
[8]P. Španěl and D. Smith, Int. J. Mass Spectrom. Ion Phys. **129**, 193 (1993) (some problems of these data for $T_{gas} = 300$ K and T_{el} above 2000 K were noted by Braun *et al.*, J. Phys. B **42**, 125202 (2009); however, these apparently are reduced by using the ratios employed in Fig. 1).
[9]S. Marienfeld, T. Sunagawa, I. I. Fabrikant, M. Braun, M.-W. Ruf, and H. Hotop, J. Chem. Phys. **124**, 154316 (2006).
[10]I. I. Fabrikant and H. Hotop, Phys. Rev. A **63**, 022706 (2001).
[11]E. E. Dashevskaya, I. Litvin, E. E. Nikitin, and J. Troe, Phys. Chem. Chem. Phys. **10**, 1270 (2008).
[12]E. E. Nikitin and J. Troe, Phys. Chem. Chem. Phys. **12**, 9011 (2010).
[13]E. I. Dashevskaya, I. Litvin, E. E. Nikitin, and J. Troe, J. Phys. Chem. A **115**, 6825 (2011).
[14]I. I. Fabrikant, H. Hotop, and M. Allan, Phys. Rev. A **71**, 022712 (2005).
[15]L. G. Gerchikov and G. F. Gribakin, Phys. Rev. A **77**, 042724 (2008).
[16]I. Rozum, N. J. Mason, and J. Tennyson, New J. Phys. **5**, 155 (2003).
[17]E. E. Nikitin and J. Troe, "On the kinetic modeling of electron attachment to polyatomic molecules," Mol. Phys. (in press).
[18]J. Troe, T. M. Miller, and A. A. Viggiano, J. Chem. Phys. **130**, 244303 (2009).
[19]*CRC Handbook of Chemistry and Physics*, 85 ed., edited by D. R. Lide (CRC, Boca Raton, 2004).
[20]N. S. Shuman, T. M. Miller, A. A. Viggiano, and J. Troe, Int. J. Mass Spectrom. **306**, 123 (2011).
[21]J.-L. Le Garrec, O. Sidko, J. L. Queffelec, S. Hamon, J. B. A. Mitchell, and B. R. Rowe, J. Chem. Phys. **107**, 54 (1997).
[22]F. Goulay, C. Rebrion-Rowe, S. Carles, J.-L. LeGarrec, and B. R. Rowe, J. Chem. Phys. **121**, 1303 (2004).
[23]E. Alge, N. G. Adams, and D. Smith, J. Phys. B **17**, 3827 (1984).
[24]R. G. Levy, S. J. Burns, and D. L. McFadden, Chem. Phys. Lett. **231**, 132 (1994).